Designer functionalized self-assembling peptide nanofiber scaffolds for growth, migration, and tubulogenesis of human umbilical vein endothelial cells

Xiumei Wang,†[ac] Akihiro Horii†[ab] and Shuguang Zhang*[a]

Received 28th April 2008, Accepted 5th August 2008
First published as an Advance Article on the web 10th September 2008
DOI: 10.1039/b807155a

We previously reported a class of designer self-assembling peptide nanofiber scaffolds as a unique biological material for diverse applications including 3-D tissue cell culture, slow drug release, regenerative medicine, and tissue engineering. One of these peptide scaffolds, RADA16-I has been used in bone, cartilage, and neural regeneration studies that have shown great promises. We here report the development of two new functionalized self-assembling peptide nanofiber scaffolds designed specifically for angiogenesis study through directly coupling pure RADA16-I with short biologically angiogenic motifs. Angiogenesis is very important in regenerative medicine. An adequate blood vessel supply to the newly formed tissue and within the transplanted scaffold is essential in determining the success of new tissue regeneration. In our study, two designer functionalized peptides, KLT, Ac–$(RADA)_4G_4$KLTWQELYQLKYKGI–$CONH_2$ and PRG, Ac–$(RADA)_4$GPRGDSGYRGDS–$CONH_2$ significantly enhanced endothelial cell survival, proliferation, migration, and morphological tubulogenesis compared with unmodified RADA16-I scaffold. We also showed in our clear-boundary sandwich culture without adding extract soluble growth factors that cells migrated uni-directionally from RADA16-I toward the functionalized scaffolds but not the reverse. Our results suggest that the functionalized designer peptide scaffolds will not only have great promise for promoting endothelial cell growth, migration, and tubulogenesis, but also may have widely potential applications for diverse tissue engineering and tissues regeneration.

1. Introduction

A class of designer self-assembling peptide nanofiber scaffolds as a unique biological material has been previously reported to have diverse and broad applications including for 3-D tissue cell culture, slow drug release, regenerative medicine, and tissue engineering.[1–5] This class of self-assembling peptide materials undergo spontaneous assembly into well-ordered interwoven nanofibers, which form hydrogels with about 10 nm fiber diameter, 5–200 nm pore size, and over 99% water content.[6] Moreover, these self-assembling peptides can be modified and functionalized by direct extension of peptides with known biologically functional peptide motifs to promote specific cellular responses. One family of these peptide scaffolds, functionalized RADA16-I (AcN–RADARADARADARADA–$CONH_2$) has been used in bone, cartilage, and neural regeneration, as well as to instantly stop bleeding and have shown great promise.[7–10]

One of the primary purposes of tissue regeneration and engineering is to develop biologically compatible substitutes that replace damaged or missing body tissues.[11] Presently inadequate vascularization developed in tissue-engineered materials has been a major obstacle for their clinical applications. Because the amount of oxygen required for cell survival is limited to a distance of approximately 200 μm from the supplying blood vessel, long-term survival and function of constructed tissue substitutes requires new blood vessels to provide nutrients and oxygen to the cells.[12,13] Therefore, an adequate blood vessel supply to the newly formed tissue and within the transplanted scaffold is thought to be essential in determining the success of new tissue regeneration. Promotion of angiogenesis in tissue engineering is always one of the major topics of tissue regeneration and tissue engineering.[14–18]

Angiogenesis refers to the formation of new capillaries from pre-existing blood vessels, which consists of several complex consecutive steps, including the stimulation of endothelial cells by growth factors, the subsequent degradation of extracellular matrix (ECM) by proteolytic enzymes, proliferation, migration and invasion of ECM of endothelial cells, and the recruitment of pericytes stabilizing the newly formed capillary network.[19,20] These steps should be considered during designing tissue-engineered scaffolds. Several kinds of scaffold materials including collagen I, fibrin, Matrigel, and PLGA sponge have previously been used for angiogenesis studies.[21–27] These studies focus on different steps of the angiogenesis process and most of them strongly depend on the supplement of soluble angiogenic growth factors. Although these biological molecules hold significant promise for developing an effective vascular system, their use may be limited in certain applications of these tissue-engineered scaffolds because of some imperative processes

[a]*Center for Biomedical Engineering, Massachusetts Institute of Technology, 77 Massachusetts Avenue, Cambridge, MA 02139, USA. E-mail: shuguang@mit.edu; Fax: +1 617-258-5239; Tel: +1 617-258-7514*
[b]*Olympus America Inc., 3500 Corporate Parkway, Center Valley, PA 18034, USA*
[c]*Biomaterials Laboratory, State Key Laboratory of New Ceramics and Fine Processing, Department of Materials Science and Engineering, Tsinghua University, Beijing 100084, China*
† X. W. and A. H. contributed equally to this paper

required for the scaffolds, such as thermal processing and sterilization. And also the applications of growth factors *in vivo* could carry high risks of hyper-stimulation and other unwanted effects.[28] Therefore, an ideal angiogenic tissue-engineered scaffold should take into account most representative steps of *in vivo* angiogenesis, not only avoid using large amount of prohibitively expensive growth factors, but also still promote capillary invasion and survival.

Recently, several peptide molecules have been reported to modulate angiogenesis.[29] RGD is a key binding sequence for cell attachment specifically working with integrins. PRGDS and YRGDS are the most commonly appearing RGD motifs in natural proteins.[30,31] Here we designed a 2-unit RGD binding sequence PRGDSGYRGDS with two similar units of RGD binding sequences, which has a higher possibility to increase cell attachment and therefore promote endothelial cell long-term survival. KLTWQELYQLKYKGI has been reported to act as a vascular endothelial growth factor (VEGF) agonist.[32] This VEGF-mimicking peptide modeled on the VEGF helix region 17–25 binds to and activates the VEGF receptors, thus activating the VEGF-dependent proliferation pathway and inducing EC proliferation. This is the only example in the literature of a synthetic peptide able to active VEGF receptors. In our study, these functionalized peptide sequences were directly extended on the self-assembling peptide RADA16-I through solid phase synthesis at the C-termini to increase the angiogenic activities of RADA16-I peptide scaffolds.

We here report an *in vitro* study of the angiogenic activities of two designer functionalized self-assembling peptide nanofiber scaffolds KLT and PRG, which significantly promote endothelial cell survival, proliferation, migration, and morphological differentiation. Our results suggest that the designer functionalized peptide scaffolds may not only have great promise for promoting endothelial cell growth, migration, and tubulogenesis, but also may be very useful for tissue engineering and diverse tissues regeneration.

2. Experimental

2.1 Peptide solution preparation and gel formation

Peptide solution preparation. All the lyophilized designer peptides used in this work were custom-synthesized by CPC Scientific (Purity >80%, San Jose, CA). These peptides were dissolved in MilliQ water at a final concentration of 1% (w/v, 10 mg ml^{-1}) and then sonicated for 30 minutes (Aquasonic, model 50T, VWR, NJ). After sonication, they were filter-sterilized (Acrodisc Syringe Filter, 0.2 μm HT Tuffrun membrane, Pall Corp., Ann Arbor, MI) for succeeding uses. The designer functionalized peptide solutions were mixed in a volume ratio of 1 : 1 with 1% pure RADA16-I solution to get 1% functionalized peptide mixtures (RAD–PRG or RAD–KLT).

Gel formation for two-dimensional (2-D) cell culture. Desired number of sterilized culture plate inserts (10 mm diameter, 0.4 μm Millicell-CM, Millipore, MA) were placed in a 24-well culture plate with 400 μl culture medium in each well. 100 μl of peptide solution (functionalized peptide mixtures or pure RADA16-I) was loaded directly into each of the inserts and then incubated for at least 1 hour at 37 °C for gelation. 400 μl of culture medium were very carefully added onto the gel and then incubated on the plate overnight at 37 °C. Once the gel was formed, the medium was carefully removed and changed twice more to equilibrate the gel to physiological PH prior to plating the cells. A certain number of cells in 400 μl of medium was seeded on the top of the gel and then the insert was moved to a new 12-well culture plate with 800 μl of medium in each well for 2-D cell culture.

Gel formation for three-dimensional (3-D) cell culture. Culture plate inserts are prepared as described above. Cells were suspended in 10% sucrose just before seeding. 20 μl of cell suspension were quickly mixed with 100 μl of peptide solution and then the mixture was added into the insert. 400 μl of medium was very carefully layered onto the gel for gelation. This was then incubated for 10 min at 37 °C and then the medium was changed for another 30 min of incubation. This was then changed twice more to equilibrate the gel to physiological pH for 3-D cell culture.

Collagen gel and matrigel formation. Rat tail collagen type I and Matrigel (growth factor-reduced lot) were purchased from BD Bioscience (Bedford, MA) and prepared according to the manufacturer's protocols. The same volume (100 μl) of collagen type I (2.5mg/ml) and Matrigel were also plated on the bottom of culture inserts and allowed to gel for 30 minutes at 37 °C, with subsequent addition of culture medium.

2.2 Cell culture of human umbilical vein endothelial cells (HUVECs)

Primary isolated HUVECs were commercially obtained from Lonza Inc. (Walkersville, MD) and routinely grown in endothelial growth media EGM-2 (Lonza Inc., Walkersville, MD) on regular tissue-culture plates. All the experiments were conducted with cells between passage 5 and passage 8. Sub-confluent ($\sim 6 \times 10^4$ cells per insert) of HUVECs was seeded on the top of the scaffolds for 2-D cell culture. About 1×10^5 of HUVECs were suspended in 100 μl of peptide solution for 3-D cell culture.

2.3 Circular dichroism (CD)

Peptide samples were prepared by diluting 1% peptides in water to a working concentration of 25 μM. Samples were analyzed at room temperature in a quartz curette with a path length of 0.5 cm and in a wavelength range 195–250 nm and the CD spectra were collected.

2.4 Fluorescence microscopy

Following the experiments, cells on the hydrogels were fixed with 4% paraformaldehyde for 15 min and permeabilized with 0.1% Triton X-100 for 5 min at room temperature. Fluorescent Rhodamin phalloidin and SYTOX® Green (Molecular Probes, Eugene, OR) were used for labeling F-actin and nuclei, respectively. Images were taken using a fluorescence microscope (Axiovert 25, ZEISS) or laser confocal scanning microscope (Olympus FV300).

2.5 DNA content measurement

The number of cells on the scaffolds was determined by the fluorometric quantification of amount of cellular DNA. The

scaffolds with cells were collected for DNA purification (QIAamp DNA Mini Kit, QIAGEN). 100 μl of purified DNA sample was mixed with 100 μl DNA binding fluorescent dye solution (0.5 μl Picogreen reagent in 100 μl TE buffer, Quant-iT™ PicoGreen dsDNA Reagent and kits, Invitrogen). The fluorescent intensity of the mixed solution was measured with a fluorescence spectrometer (Wallace Victor2, 1420 Multi-label counter, excitation at 485nm and emission at 510nm, Perkin-Elmer, MA).

2.6 Boundary-sandwiched cell migration assay

Peptide scaffolds were prepared as described above. A schematic illustration of boundary-sandwiched cell migration assay is shown in Fig. 4B image (a). Approximately 8×10^4 cells were seeded on the top of peptide scaffold A and then incubated for 6 hours at 37 °C with 5% CO_2 for cell attachment. Trimmed quadrate peptide scaffold A with attached cells was inversely placed on the surface of peptide scaffold B with cells between two types of scaffolds. The scaffolds with cells were cultured at 37 °C for 2 days and then examined with fluorescence microscopy after nuclei staining.

2.7 Statistical analysis

All the data were statistically analyzed to express in the standard deviation of the mean. The t-test was performed and $p < 0.01$ was commonly accepted to be statistically significant.

3. Results and discussion

3.1 Self-assembly of designer functionalized peptides

The designer peptides sequences and descriptions are listed in Table 1. These designer peptides PRG and KLT were synthesized by direct extension from the C-terminal of the self-assembling peptide RADA16-I using solid phase synthesis with different functional peptide motifs (Fig. 1a). They were selected from the functional domains on several extracellular matrix proteins and cytokines that are shown to have angiogenic activities and promote endothelial cell adhesion, proliferation, and migration. Glycine residues were used between the self-assembling motif $(RADA)_4$ and the functional motif as a space linker for keeping the flexibility of functional peptides. The pure functionalized peptide PRG or KLT undergoes very weak self-assembly and forms a very soft hydrogel, which is difficult to handle for cell culture. Mixing with self-assembling peptide RADA16-I facilitated their self-assembly and gelation. The most possible reason is that the functionalized peptide interact with RADA16-I through the self-assembling motif $(RADA)_4$. A schematic illustration is shown in Fig. 1b.

Table 1 Designer self-assembling peptides used in this study

Code	Sequences	Description
RADA16-I	Ac–$(RADA)_4$–$CONH_2$	Designer self-assembling motif
PRG	Ac–$(RADA)_4$ GPRGDSGYRGDS–$CONH_2$	2-unit RGD motif
KLT	Ac–$(RADA)_4G_4$ KLTWQELYQLKYKGI–$CONH_2$	Mimicking VEGF helix region, activate VEGF receptors

Our previous studies have shown that the formation of stable beta-sheet is very important and necessary for peptides self-assembly and nanofiber formation. CD spectra were used to assess the presence of beta-sheets in RADA16-I and peptide mixtures. A typical spectrum for beta-sheet structures with a minimum mole residue ellipticity at 215 nm and a maximum at 195 nm was observed for our peptides studies. These functionalized peptide mixtures exhibited similar structural properties to the RADA16-I sequence (Fig. 1e). The addition of functional motif sequences reduced the beta-sheet content of the peptide mixtures, as shown by a decrease in the intensity of mole residue ellipticity at 215 nm.

Scanning electron microscopy (SEM) and Atomic Force Microscopy (AFM) examinations also confirm the self-assembling nanofiber formations. As shown in Fig. 1c and Fig. 1d, uniform and interweaved long nanofibers can be observed in the functionalized peptide mixtures, which suggest that the functionalized peptides interact with RADA16-I and incorporate into the nanofibers quite well. We have also investigated the variations in the nanofiber morphologies and diameters of the functionalized peptide mixtures as compared with RADA16-I, which also implied the incorporation in these functionalized peptide mixtures.[9]

3.2 Cell attachment and viability

In order to evaluate the HUVECs viabilities on these functionalized peptide scaffolds, the same number of cells were seeded on the top of the different scaffolds and cultured for two days. Type I collagen gel was used as a positive control. Fig. 2 showed the typical morphologies of HUVECs on different scaffolds. The seeded HUVECs exhibit good attachment and higher viability on collagen I, RAD–PRG and RAD–KLT, whereas RADA16-I was less effective for maintaining cell survival. Beyond that, the cell morphology on RAD–PRG is quite similar with that on collagen gel, suggesting the RGD units in the PRG peptide significantly increase the HUVECs attachment and viability.

3.3 Cell proliferation

We also estimated cell growth on these peptide scaffolds by examining DNA contents extracted from the scaffolds after 6-hour, 1-day, 2-day, and 3-day culture (Fig. 3). The differences in DNA contents among different scaffolds can be used to estimate the cell numbers. Cells attached on these scaffolds after 6-hour culture showed a better adhesion on the scaffold RAD–PRG. Furthermore, we noted that cells on RADA16-I started proliferating after 2 days, while they proliferated after 1 day on scaffolds RAD–KLT and RAD–PRG. Beyond that, the cell numbers on RAD–PRG and RAD–KLT were about 1.5 times as many as that on RADA16-I. These results suggested that the cells behavior was positively affected by the functional motifs of PRG and KLT. In contrast, low cell numbers on RADA16-I indicated the low proliferation rates or low cell viabilities. This proliferation was also consistent with the morphologic observations from fluorescence microscopy examinations.

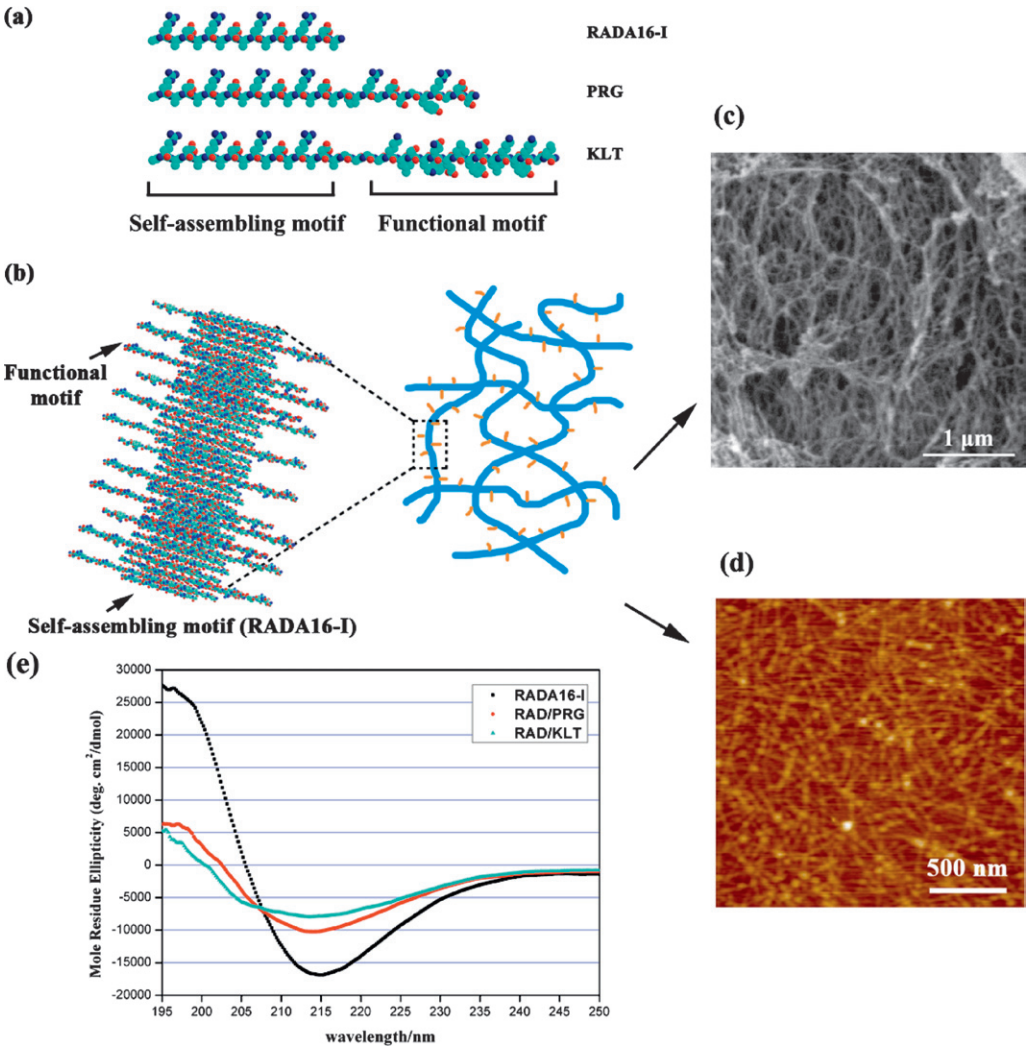

Fig. 1 Molecular models of designer peptides and schematic illustrations of self-assembling peptide nanofiber scaffolds. (a) Molecular modes of designer peptides RADA16-I, PRG, and KLT. (b) Schematic illustrations of self-assembling peptide nanofibers formation after mixing RADA16-I with PRG peptides, representing a β-sheet double-tape structure. Hydrophobic alanine side groups are present on one side of self-assembling motif RADA16-I β-sheet and the other side is populated with alternating positive and negative charges due to the arginine and aspartic acid residues, respectively. The functional motifs extrude from nanofiber backbones. (c) Typical SEM morphology of the functionalized peptides nanofiber scaffold. (d) Typical AFM image of self-assembling functionalized peptides solutions. (e) Typical CD spectrum of RADA16-I with high beta-sheet content and the mixtures with functionalized peptides, the two additional spectra (red and teal) show considerably less beta-sheet contents.

Angiogenesis strongly depends on the maintenance of endothelial cell viability and inhibition of endothelial cell apoptosis.[33] Endothelial cell long-term survival is thought to be essential during angiogenesis. Previous studies have shown that many of angiogenic growth factors inhibit endothelial cell apoptosis[34–36] and the adhesion of endothelial cells to the extracellular matrix promotes endothelial cell survival.[37,38] The functional motif of PRG with two units of RGD binding sequences may have a higher tendency to increase cell attachment and therefore promotes endothelial cell survival. The functional motif of KLT acts as a VEGF agonist, thus inducing endothelial cell proliferation and inhibiting endothelial cell apoptosis. Therefore, designer functionalized self-assembling peptides PRG and KLT have a potentially great value for promoting angiogenesis process *in vitro* and perhaps *in vivo* as well. It will be interesting to combining both PRG and KLT together as a multi-function scaffold. Further systematic experiments will address this question.

3.4 Cell Migration

In order to study the preferences of endothelial cells migration in response to the components of surrounded scaffolds and the importance of functional peptide motif for guiding cells migration, we designed the clear-boundary sandwich assays to assess endothelial cell migration between two types of peptide scaffolds. As shown in Fig. 4B, endothelial cells plated on the scaffolds RAD–PRG (Fig. 4B, images a and e) and RAD–KLT (Fig. 4B, images b and f) settled in these scaffolds and no visible migration towards RADA16-I scaffold was observed. In contrast, cells seeded on RADA16-I scaffold directionally migrated towards functionalized peptide scaffolds (Fig. 4B, images c, d, g and h).

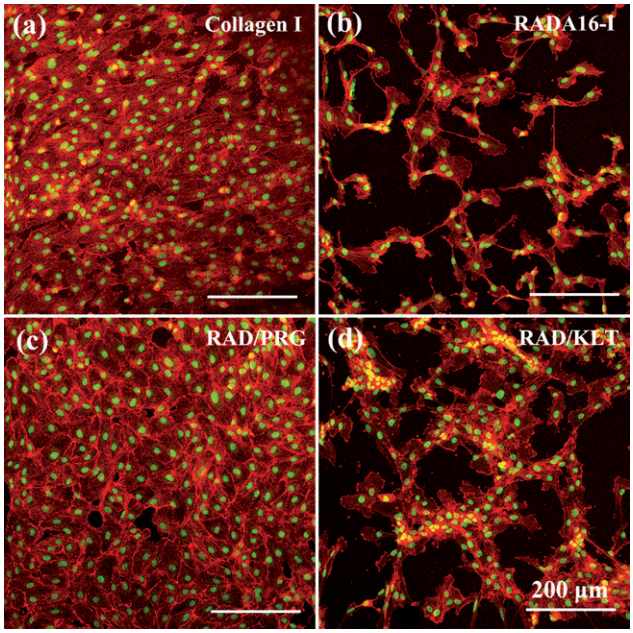

Fig. 2 Fluorescence microscopy images of HUVECs morphology on different peptide scaffolds with collagen-I gel as a positive control after 2-day culture. Fluorescent staining with Rhodamin phalloidin for F-actin (red) and SYTOX Green for nuclei (green) showed the cell attachments and viabilities. The scale bar represents 200 μm for all panels.

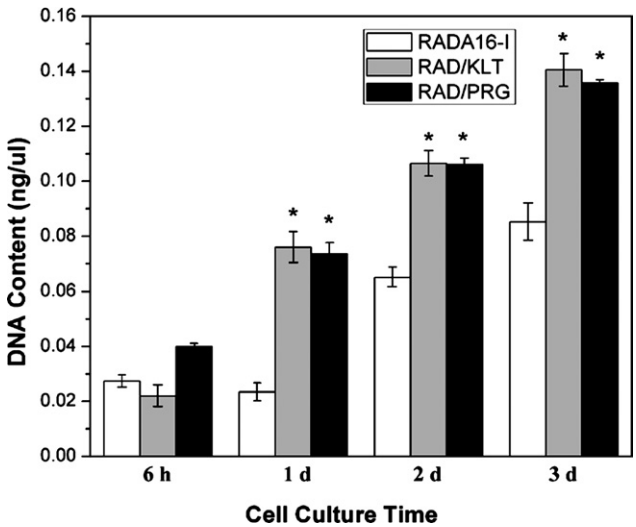

Fig. 3 Endothelial cell proliferation on different kinds of peptide scaffolds. Cell numbers are evaluated by DNA content measurement from various scaffolds after cell culture for 6 hours, 1 day, 2 days and 3 days. Cell numbers cultured on functionalized peptide scaffolds RAD–PRG and RAD–KLT were statistically higher than that on pure RADA16-I scaffolds (*$p < 0.01$, t-test).

These experiments unambiguously show the biological importance of the designer functionalized peptide scaffolds that induce cell directional migrations. This is a very important observation since there are no additional soluble growth factors in these scaffolds. These observations suggest the adhesion peptide motif alone can induce cell migration without extract soluble factors.

Many factors are involved in cell unidirectional migration, such as soluble chemoattractants,[39] attachment on surrounding matrix,[40,41] and perhaps more. In literature reports, endothelial cell migration is mostly stimulated by growth factors such as VEGF and bFGF, and also is activated in response to integrins binding to ECM component. Our results demonstrated unequivocally that the adhesive interactions governed mainly by the functional motif of PRG alone promote cell attachment and migration from RADA16-I to RAD–PRG scaffold, whereas the VEGF mimicking sequence of KLT may mainly serve the similar function of VEGF to regulate endothelial cell migration. Cells seeded on RADA16-I were probably induced by the functional motifs of PRG and KLT and migrated to/on these functionalized peptide mixtures scaffolds (Fig. 4A, image b). More systematic experiments will be carried out to further address these questions.

3.5 Capillary-like structures formation in 2-D and 3-D models

In the literature, most of the two-dimensional angiogenesis models where endothelial cells seeded on flat surfaces form capillary-like structure under certain conditions in a network pattern with central voids, which mimic vessel wall and lumen.[42,43] In our study, in order to determine if the functional peptide motifs assembled in the peptide scaffolds could facilitate the formation of capillary-like structure without supplement of extra growth factors in EGM-2, sub-confluent monolayer cells were plated on the surfaces of scaffolds, 1) RAD–PRG, 2) RAD–KLT, 3) collagen-I and 4) Matrigel for cell cultures up to 1 week.

The typical morphologies of cell organizations after 1-day culture are shown in Fig. 5. It can be clearly seen that HUVECs formed capillary-like structure networks on RAD–KLT and Matrigel (Fig 5). Whereas no cell networks formation were observed on RAD–PRG, on which cells formed uniformed attachment similar with those on collagen-I gel (Fig.5). To further determine the time needed for formation of capillary-like structure and sequential capillary-like structure morphology changes, cells from 4-hour and 3-day cultures were also examined. The morphology examinations revealed that the capillary-like structure networks started from 4 hours after seeding and continued to 3 days (results not shown). We have also observed the morphologies under the confluent-seeding conditions. Similar capillary-like structure networks were also observed on RAD–KLT and Matrigel scaffolds (results not shown).

In most *in vitro* angiogenesis models, endothelial cells undergo morphological differentiation and reorganize into an extensive network of capillary like structure in both short-term and long-term cultures depending on matrix and culture conditions.[43] In our current studies, HUVECs seeded on designer RAD–KLT scaffold rearranged into capillary-like structure network as early as 4 h after seeding and remained intact for up to 3 days, very similar to cell behaviors in Matrigel. It is known that Matrigel contains many growth factors that stimulate capillary-like structure formation rapidly. In our study, no extra soluble growth factors were added to the RAD–KLT scaffold. This observation is very significant and suggests that capillary-like structure formation does not completely depend on soluble factors alone, but the permissive and stimulating scaffolds play a vital role for angiogenesis. The coupled functional peptide

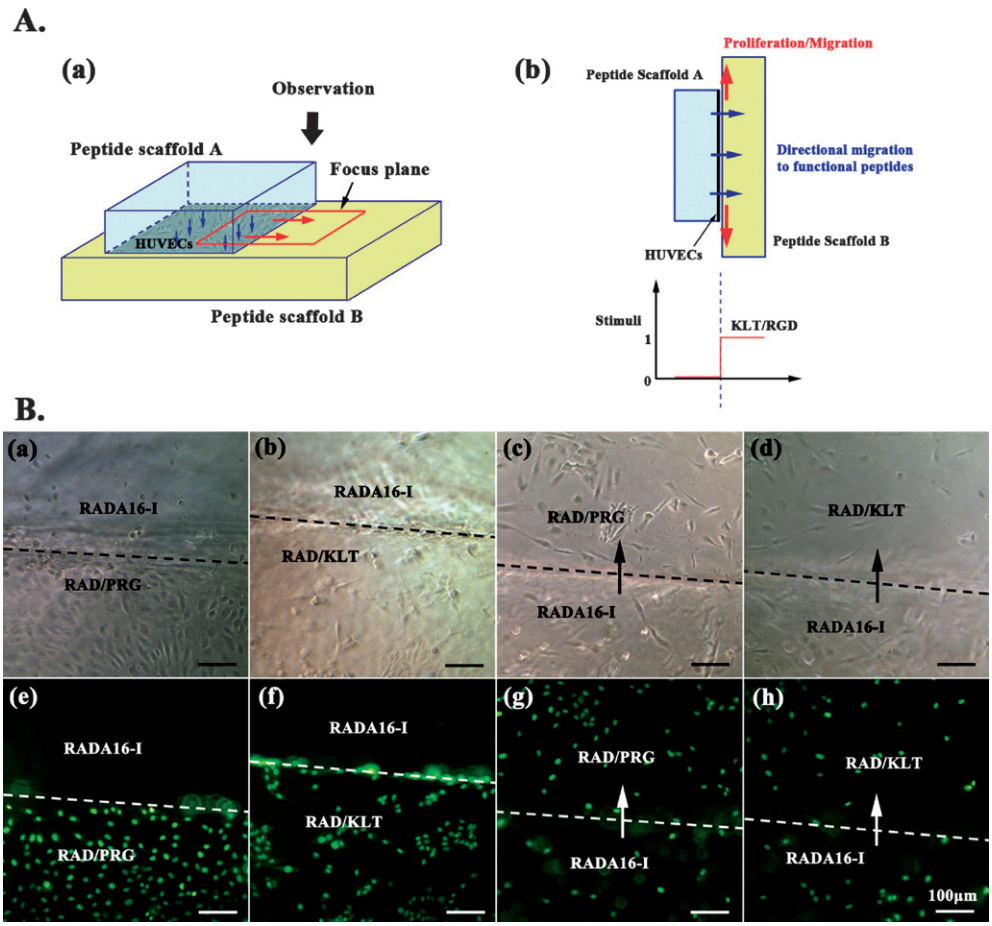

Fig. 4 Endothelial Cell unidirectional migration in responds to functional peptide scaffolds. A) Schematic illustrations of cell directional migration. a) Clear-boundary sandwich cell migration assay. b) Directional migration induced by functional motifs. B) Phase contrast microscopy images of HUVECs seeded on peptide scaffolds: a) RAD–PRG; b) RAD–KLT; c) and d) RADA16-I, and fluorescent SYTOX Green nuclear staining for e) RAD–PRG; f) RAD–KLT; g) and h) RADA16-I. Cells directionally migrated from RADA16-I to RAD–PRG (c and g) and RAD–KLT (d and h). The scale bar represents 100 μm for all panels.

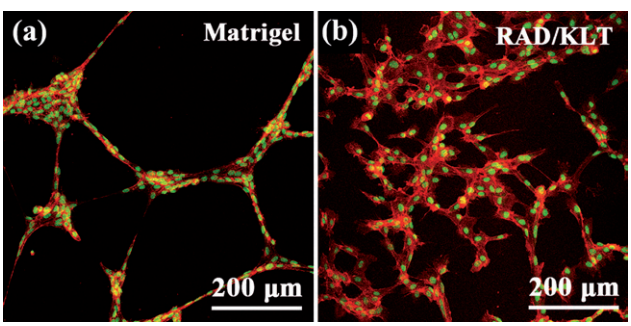

Fig. 5 Capillary-like structure networks formation on RAD–KLT peptide scaffold after 1-day culture. (a) Matrigel; (b) RAD–KLT.

motif of KLT showed stimulating effects similar to soluble growth factor to promote endothelial cell differentiation.

In short-term models, cells sub-confluence was thought to be necessary for capillary-like structure formation. However in our study, capillary-like structure formation on RAD–KLT and Matrigel does not entirely depend on cell-seeding density. RAD–KLT scaffold containing VEGF-mimicking motif quickly induced formation of capillary-like structure network independent of cell numbers and other soluble growth factors. This is another important observation.

In addition to 2-D culture, we uniformly encapsulated HUVECs into the peptide scaffolds for 3-D cell culture. In this study 20 ng ml^{-1} of VEGF were added into the EGM-2 to keep the cells long-term survival (up to 1 week) and to induced cell differentiation. All types of peptide samples were examined by laser confocal scanning microscopy after one-day culture. The typical cell morphologies and 3-D reconstructions were shown in Fig. 6. Firstly, it is observed that endothelial cells in 3-D environment were elongated with many cellular protrusions rather than the characteristic cobblestone and flattened morphology. Secondly, endothelial cells also displayed diverse morphologies in response to different surrounding peptide matrix. They adopted a more spread shape in functionalized peptide scaffolds than in pure RADA16-I scaffold. Finally, the 3-D reconstructions clearly showed that the cells elongated to find each other to form cellular connections, which suggested that all these three types of peptide scaffolds have provided suitable 3-D environments for endothelial cells growth and differentiation. After 1-week culture, differentiated endothelial cells underwent

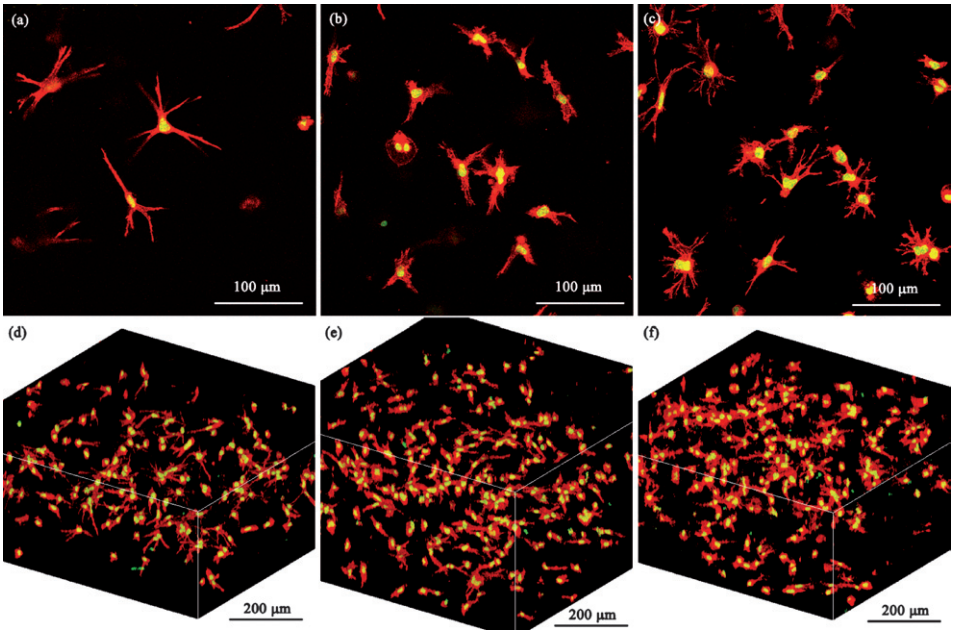

Fig. 6 Endothelial cell morphologies in 3-D peptide scaffolds. Laser confocal scanning microscopy images of HUVECs in (a) Pure RADA16-I; (b) RAD–PRG; (c) RAD–KLT. (d)–(f) Related 3D constructions of the cell morphologies in 3-D peptide scaffolds. The green stain shows nuclei, the red stain shows actin fiber. VEGF (20 ng ml^{-1}) was added to the cell culture medium and the cells were cultured for 1 day.

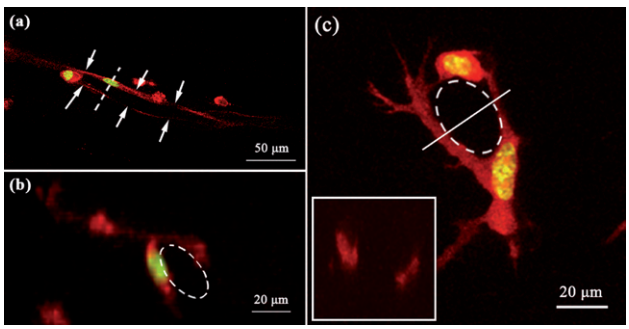

Fig. 7 Tubulogenesis in 3D cell culture. (a) Lumen formation (arrows) of HUVECs in 3D RAD–PRG scaffold shown by fluorescence confocal microscopy. (b) Reconstructed image of the cross-section at the dotted line in (a). The capillary lumen was also shown in the cross-section image (dotted circle). (c) Capillary-like structure formation in 3-D RADA16-I scaffold. Dotted circle in (c) showed the lumen formation. The reconstructed image of the cross-section at the real line in (c) was shown in the lower left corner of (c), which showed the lateral view of the tubular wall. The green stain shows nuclei, the red stain shows actin fiber. VEGF (20 ng ml^{-1}) was added to the cell culture medium and the cells were cultured for up to 7 days.

tubulogenesis and formed capillary-like structure, as shown in Fig. 7. In this study, both pure RADA16-I and functionalized peptide scaffolds could facilitate cells to form capillary-like structures through cellular reorganization of one cell (Fig. 7, image a and b) or cellular connection of two or more cells (Fig. 7, image c). No significant differences were observed among these peptide scaffolds, which indicated that all peptides scaffolds could provide suitable environments for endothelial cell growth and induce differentiation with addition of VEGF. Fig. 7 presented the typical examples of tubulogenesis in 3-D peptide scaffolds.

3.6 Other implications

Increasing numbers of *in vitro* angiogenesis models have been developed and reported in the literature after angiogenesis was first observed *in vitro* in 1980.[42] These angiogenesis models can be roughly classified into 2-D and 3-D models. They have not only significantly increased our understanding of physiological and pathological angiogenesis processes, but also they have been used to screen angiogenic and angiostatic molecules.[43] The 2-D models are simplistic and mainly designed for the role of ECM in vascular morphogenesis, *in vitro* activity of angiostatic molecules, and the ultra-structure of capillary-like structure. However, 2-D models lack the third dimension and thus they cannot truly reflect all steps of angiogenesis. The 3-D models are more realistic and appropriate for studying sprouting angiogenesis, effects of cytokines, and other cell behavioral phenomena. In most 3-D systems, high concentrations of angiogenic factors are required for cell survival and sprouting because cultured endothelial cells undergo apoptosis ~28–72 hours after seeding.

In our current study, we mainly focus on angiogenesis for tissue engineering and tissue regeneration, especially for designing and selecting ideal tissue-engineered scaffolds that promote endothelial cell long-term survival, proliferation, migration, differentiation, and capillary invasion. 2-D and 3-D angiogenesis models are therefore both necessary for studying the different cellular responses of endothelial cells to the designer biological materials. Although we have also studied endothelial cell morphogenesis, and lumen formation in 3-D designer functionalized peptide scaffolds, more systematic 3-D studies will be further investigated in detail in subsequent study.

In addition to *in vitro* studies, full analysis of blood vessel in-growth in engineered tissue substitutes *in vivo* is necessary for

comprehensive understanding of the effects and applications of biological scaffolds in tissue regeneration. We have also carried out biologically chorioallantoic membrane assay, which is a commonly used *in vivo* model to study angiogenesis, we will assess the efficiency *in vivo* of various designer peptide scaffolds in inducing capillary invasion in a separate report.

4. Conclusion

We have developed and evaluated two new designer functionalized self-assembling peptide nanofiber scaffolds specifically for angiogenesis study through directly coupling RADA16-I with short biologically angiogenic motifs. In our study, these two designer functionalized peptides, KLT and PRG have been demonstrated to significantly enhance endothelial cell survival, rapid proliferation, migration, and morphological differentiation *in vitro*. These scaffolds will be likely very useful for tissue engineering and diverse tissues regenerations.

Acknowledgements

This work was primarily supported by Olympus Corporation.

References

1 S. Zhang, *Nat. Biotechnol.*, 2003, **21**, 1171–1178.
2 S. Zhang, T. C. Holmes, C. Lockshin and A. Rich, *Proc. Natl. Acad. Sci. U. S. A.*, 1993, **90**, 3334–3338.
3 S. Zhang, T. C. Holmes, C. M. Dipersio, R. O. Hynes, X. Su and A. Rich, *Biomaterials*, 1995, **16**, 1385–1393.
4 Y. Nagai, L. D. Unsworth, S. Koutsopoulos and S. Zhang, *J. Controlled Release*, 2006, **115**, 18–25.
5 J. Kisiday, M. Jin, B. Kurz, H. Hung, C. Semino, S. Zhang and A. J. Grodzinsky, *Proc. Natl. Acad. Sci. U. S. A.*, 2002, **99**, 9996–10001.
6 H. Yokoi, T. Kinoshita and S. G. Zhang, *Proc. Natl. Acad. Sci. U. S. A.*, 2005, **102**, 8414–8419.
7 R. G. Ellis-Behnke, Y. X. Liang, S. W. You, D. Tay, S. Zhang, F. K. So and G. Schneider, *Proc. Natl. Acad. Sci. U. S. A.*, 2006, **103**, 5054–5059.
8 F. Gelain, D. Bottai, A. Vescovi and S. Zhang, *PLoS One*, 2006, **1**, e119.
9 A. Horii, X. M. Wang, F. Gelain and S. Zhang, *PLoS One*, 2007, **2**, e190.
10 R. G. Ellis-Behnke, Y. X. Liang, D. K. C. Tay, P. W. F. Kau, G. E. Schneider, S. Zhang, W. Wu and K. F. So, *Nanomed., Nanotechnol., Biol. Med.*, 2007, **2**, 207–215.
11 R. Langer and J. P. Vacanti, *Science*, 1993, **260**, 920–926.
12 C. K. Colton, *Cell Transplant.*, 1995, **4**, 415–436.
13 D. J. Mooney and A. G. Mikos, *Sci. Am.*, 1999, **280**, 60–65.
14 K. A. Wieghaus, S. M. Capitosti, C. R. Anderson, R. J. Price, B. R. Blackman, M. L. Brown and E. A. Botchwey, *Tissue Eng.*, 2006, **12**, 1903–1913.
15 S. Soker, M. Machado and A. Atala, *World J. Urol.*, 2000, **18**, 10–18.
16 M. W. Laschke, Y. Harder, M. Amon, I. Martin, J. Farhadi, A. Ring, N. Torio-Padron, R. Schramm, M. Rucker, D. Junker, J. M. Häufel, C. Carvalho, M. Heberer, G. Germann, B. Vollmar and M. D. Menger, *Tissue Eng.*, 2006, **12**, 2093–2104.
17 E. J. Suuronen, L. Muzakare, C. J. Doillon, V. Kapila, F. Li, M. Ruel and M. Griffith, *Int. J. Artif. Organs*, 2006, **29**, 1148–1157.
18 A. Wenger, A. Stahl, H. Weber, G. Finkenzeller, H. G. Augustin, G. B. Stark and U. Kneser, *Tissue Eng.*, 2004, **10**, 1536–1547.
19 W. Risau, *Nature*, 1997, **386**, 671–674.
20 P. Carmeliet, *Nat. Med.*, 2000, **6**, 389–395.
21 T. L. Bach, C. Barsigian, D. G. Chalupowicz, D. Busler, C. H. Yaen, D. S. Grant and J. Martinez, *Exp. Cell Res.*, 1998, 238.
22 G. E. Davis and C. W. Camarillo, *Exp. Cell Res.*, 1996, **224**, 39–51.
23 M. N. Nakatsu, R. C. A. Sainson, J. N. Aoto, K. L. Taylor, M. Aitkenhead, S. Pérez-del-Pulgar, P. M. Carpenter and C. C. W. Hughes, *Microvasc. Res.*, 2003, **66**, 102–112.
24 A. E. Elcin and Y. M. Elcin, *Tissue Eng.*, 2006, **12**, 959–968.
25 M. C. Ford, J. P. Bertram, S. R. Hynes, M. Michaud, Q. Li, M. Young, S. S. Segal, J. A. Madri and E. B. Lavik, *Proc. Natl. Acad. Sci. U. S. A.*, 2006, **103**, 2512–2517.
26 D. A. Narmoneva, O. Oni, A. L. Sieminski, S. Zhang, J. P. Gertler, R. D. Kamm and R. T. Lee, *Biomaterials*, 2005, **26**, 4837–4846.
27 M. E. Davis, J. P. M. Motion, D. A. Narmoneva, T. Takahashi, D. Hakuno, R. D. Kamm, S. Zhang and R. T. Lee, *Circulation*, 2005, **111**, 442–450.
28 R. J. Lee, M. L. Springer, W. E. Blanco-Bose, R. Shaw, P. C. Ursell and H. M. Blau, *Circulation*, 2000, **102**, 898–901.
29 L. D. D'Andrea, A. D. Gatto, C. Pedone and E. Benedetti, *Chem. Biol. Drug Des.*, 2006, **67**, 115–126.
30 S. Kouvroukoglou, K. C. Dee, R. Bizios, L. V. McIntire and K. Zygourakis, *Biomaterials*, 2000, **21**, 1725–1733.
31 M. S. Aguzzi, C. Giampietri, F. D. Marchis, F. Padula, R. Gaeta, G. Ragone, M. C. Capogrossi and A. Facchiano, *Blood*, 2004, **103**, 4180–4187.
32 L. D. D'Andrea, G. Laccarino, R. Fattorusso, D. Sorriento, C. Carannante, D. Capasso, B. Trimarco and C. Pedone, *Proc. Natl. Acad. Sci. U. S. A.*, 2005, **102**, 14215–14220.
33 E. Chavakis and S. Dimmeler, *Arterioscler. Thromb. Vasc. Biol.*, 2002, **22**, 887–893.
34 T. Alon, I. Hemo, A. Itin, J. Pe'er, J. Stone and E. Keshet, *Nat. Med.*, 1995, **1**, 1024–1028.
35 H. J. Kwak, J. N. So, S. J. Lee, I. Kim and G. Y. Koh, *FEBS Lett.*, 1999, **448**, 249–253.
36 A. Karsan, E. Yee, G. G. Poirier, P. Zhou, R. Craig and J. M. Harlan, *Am. J. Pathol.*, 1997, **151**, 1775–1784.
37 J. E. Meredith, B. Fazeli and M. A. Schwartz, *Mol. Biol. Cell*, 1993, **4**, 953–961.
38 S. Stromblad and D. A. Cheresh, *Chem. Biol.*, 1996, **3**, 881–885.
39 L. Lamalice, F. L. Boeuf and J. Huot, *Circ. Res.*, 2007, **100**, 782–794.
40 V. Nehls, R. Herrmann and M. Huhnken, *Histochem. Cell Biol.*, 1998, **109**, 319–329.
41 R. L. Klemke, S. Cai, A. L. Giannini, P. J. Gallagher, P. de Lanerolle and D. A. Cheresh, *J. Cell Biol.*, 1997, **137**, 481–492.
42 J. Folkman and C. Haudenschild, *Nature*, 1980, **288**, 551–556.
43 B. Vailhe, D. Vittet and J. J. Feige, *Lab. Invest.*, 2001, **81**, 439–452.